Available online at www.sciencedirect.com
SCIENCE DIRECT®
International Journal of Mass Spectrometry 242 (2005) 169–182
International Journal of Mass Spectrometry
www.elsevier.com/locate/ijms

Review

Isotope ratio measurements by secondary ion mass spectrometry (SIMS) and glow discharge mass spectrometry (GDMS)

Maria Betti *

European Commission, Joint Research Centre, Institute for Transuranium Elements, P.O. Box 2340, 76125 Karlsruhe, Germany

Received 5 September 2004; accepted 22 November 2004

Abstract

The basic principles of secondary ion mass spectrometry and glow discharge mass spectrometry have been shortly revisited. The applications of both techniques as exploited for the isotope ratio measurements in several matrices have been reviewed. Emphasis has been given to research fields in expansions such as solar system studies, medicine, biology, environment and nuclear forensic.

The characteristics of the two techniques are discussed in terms of sensitivity and methodology of quantification. Considerations on the different detection possibilities in SIMS are also presented.

Keywords: Secondary ion mass spectrometry; Glow discharge mass spectrometry, Isotope ratios; Geology; Environment

Contents

* Tel.: +49 7247 951 363; fax: +49 7247 951 186.
E-mail addresses: betti@itu.fzk.de, maria.betti@cec.eu.int (M. Betti).

1387-3806/$ – see front matter © 2004 Elsevier B.V. All rights reserved.
doi:10.1016/j.ijms.2004.11.022

1. Introduction

One of the main characteristics of mass spectrometry is its possibility for determining isotopic abundance. Precise and accurate isotope ratio measurements are of high importance in several fields of research and applications [1–5]. For instance, the measurements of stable isotopes in nature are exploited to investigate their variation and/or age dating. Isotope ratios of radiogenic elements are of extreme interest in nuclear industry; quality assurance of nuclear fuel materials and radioactive waste control. Other fields of research where isotope ratio measurements play an extremely important role are: nuclear safeguards of clandestine nuclear activities; monitoring of radioactivity in the environment during routine operations as well as in case of radiological alarm. Moreover, many applications in medicine and biology are based on the knowledge of isotope ratios.

Glow discharge mass spectrometry (GDMS) and secondary ion mass spectrometry (SIMS) are both solid mass spectrometric techniques. However, they differ in several characteristics, for instance the ionisation and atomisation mechanisms, the detection mode (imaging detection in SIMS), the capability to analyse microstructure or microparticles. In some recent publications the reader can find these techniques described [6–10]. However, the general principles of both methods will be briefly reviewed in this article. Then focus will be on the exploitation of SIMS and GDMS for the isotopic ratio measurements in different matrices and fields of research and applications. Due to the large variation of applications, this review does not pretend to be exhaustive of all available literature and considers mostly the developments during the last 5 years emphasising the most challenging research fields.

2. Secondary ion mass spectrometry

Secondary ion mass spectrometry (SIMS) is based on the mass spectrometry of ionised particles that are emitted when a surface, usually a solid, is bombarded by energetic primary particles, which may be electrons, ions, neutrals or photons. The emitted or "secondary" particles will be electrons, neutral species, atoms or molecules, or atomic and cluster ions. The large majority of species emitted are neutral, but it is the secondary ions that are detected and analysed by the mass spectrometer. This is a process that provides a mass spectrum of a surface and enables a detailed chemical analysis of a surface or solid to be performed.

Today, SIMS has an acknowledged place among the major techniques of surface analysis and micro-structural characterisation of solids. Static SIMS emerged as a technique of potential importance in the late 1960s and early 1970s as a consequence of the work of Benninghoven and his group in Münster. Whilst the SIMS technique is basically destructive, the Münster group demonstrated that using a very low primary particle flux density (<1 nA cm^{-2}) spectral data could be generated in a time scale which is very short compared to the lifetime of the surface layer.

On the other hand, the technique is known as dynamic SIMS due to its destructive capability to analyse the elemental composition of materials as a function of depth. Dynamic SIMS has found extensive application throughout the semiconductor industry where the technique had a unique capability to identify chemically the ultra-low levels of charge carriers in semiconductor materials and to characterise the layer structure of devices.

SIMS is particularly noted for its outstanding sensitivity of chemical and isotopic detection. Quantitative or semi-quantitative analysis can be performed for small concentrations of most elements in the periodic table, including the lightest. However, the high versatility of SIMS is mainly due to the combination of high sensitivity with good topographic resolution, both in depth and (for imaging SIMS) laterally. It is generally superior trace element sensitivity, capability for spatial resolution in three dimensions and for isotope measurements, as well as potential for identification of chemical compounds in many cases, make SIMS one of the preferred methods for the solution of an analytical problem.

Deficiencies, however, still exist in the capability of SIMS for quantitative elemental analyses compared to other surface techniques (Auger, X-ray photoelectron spectroscopy, electron microprobe techniques, etc.). These deficiencies can be traced to the extreme dependence of relative and absolute secondary ion yields on several parameters. Among these the following are the most important:

- matrix effects;
- surface coverage of reactive elements;
- angle of incidence of primary beam with respect to the sample surface;
- angle of emission of detected ions;
- mass-dependent transmission of the mass spectrometer;
- energy band-pass of the mass spectrometer;
- dependence of detector efficiency on element.

Quantitative elemental SIMS analysis poses a twofold problem. Firstly, spectral interpretation, namely, the extraction of total detected isotopic ion currents assignable to elemental and molecular ions from a complete SIMS spectrum of the sample; secondly, spectral quantification, namely the calculation of elemental concentration from total isotopic elemental (and molecular) ion currents. Difficulties in spectral interpretation are considerably reduced if high resolution

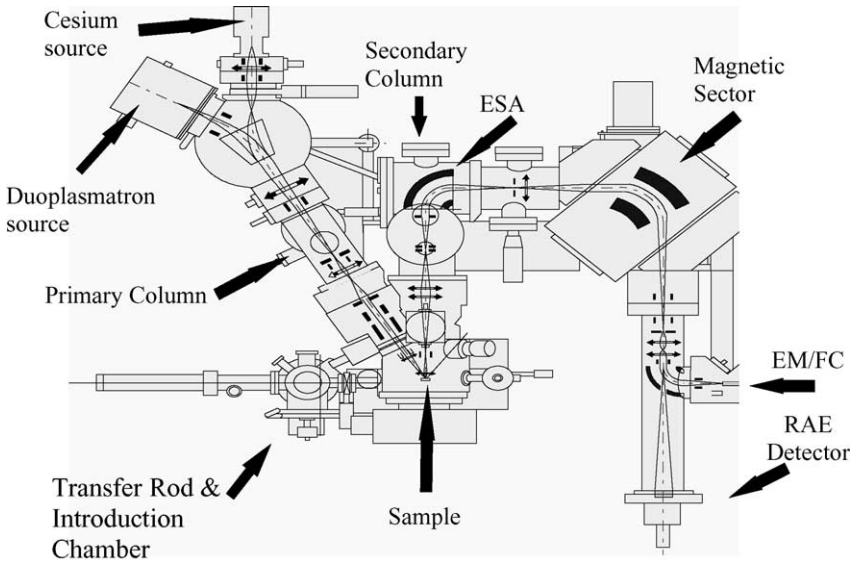

Fig. 1. Diagram of a double focusing SIMS [76] (reproduced with permission). RAE is a resistive anode encoder. ESA is the electrostatic sector positioned on the trajectory of the secondary ions (travelling in the secondary column) before the magnetic sector. FC and EM are the Faraday cup and the electron multiplier.

mass analysers ($M/\Delta M > 3000$) are used for mass analysis of secondary ions because most of the commonly occurring isotopic and molecular interferences (e.g., hydrocarbons, oxides, hydrides) can be resolved.

2.1. Practical principles

A diagram of a SIMS instrument with double-focusing mass analyser is represented in Fig. 1. Secondary ion mass spectrometry is based on:

- bombardment of the sample surface by focused primary ions, with sputtering of the outmost atomic layers;
- mass spectrometric separation of the ionised secondary species (sputtered atoms, molecules, clusters) according the their mass-to-charge ratios;
- collection of separated secondary ions as quantifiable mass spectra, as in-depth or along-surface profiles, or as distribution images of the sputtered surface.

The primary ions are normally produced by a duoplasmatron type of gas source such as O_2^+, O^-, N_2^+, Ar^+; by surface ionisation as for Cs^+ and Rb^+; or by liquid-metal field ion emission as Ga^+ and In^+. The most common primary ions used are the oxygen ions, Cs^+ and Ga^+. The ions are accelerated and focused to a selected impact area on the specimen. The collision cascade following the incidence of a primary ion results in the implantation of the primary particle, reshuffling of some 50–500 matrix atoms, and emission of secondary particles, neutral or ionised. Secondary ions from the specimen are extracted into the mass spectrometer, which can consist of electric (ESA)/magnetic deflection fields or be of the quadrupole or time-of-flight design. Secondary ions with a given mass-to-charge ratio and within a certain interval of kinetic energy are collected for pulse or current measurement, ion-optic imaging, and data processing. Of particular interest is the use of the resistive anode encoder (RAE) as detector. It is used for the analysis of microparticles and has the advantage that single-ion events are detected digitally. It therefore delivers quantitative results, irrespective of local differences in the amplification of the channel plate. One disadvantage is that the counting rate is limited to 200,000.

The different ways of operating a SIMS instrument are presented in Fig. 2. In the microscope mode, a defocused primary ion beam (5–300 μm) is used for investigating a large surface. The secondary ions are then transmitted to the mass spectrometer and generally imaging detected. In the microprobe mode, a focused primary ion beam (<10 μm) is used for investigating a very small portion of the surface and detecting inclusions in bulk material. The lateral resolution is defined by the primary ion beam size. In this case, as detector is usually employed an electron multiplier.

2.2. Sensitivity and quantification

Fig. 3 shows schematically the types of analytical information that can be obtained by SIMS analysis. A SIMS spectrum normally shows mass peaks that are characteristic of the sputtered solid but affected by experimental factors. For instance, among these factors the following should be mentioned: type, intensity, energy and incidence angle of the primary ions; the transmission of the secondary ions and the selectivity for them in the mass analyser; the type of detector. There are, effectively, two spectra: that of the matrix and that of the impurities.

The task of analytical SIMS is to quantify the secondary ion currents, that is to convert the intensity of one or several peaks characteristic of an element to its corresponding concentration c_e. When a primary ion beam with a current den-

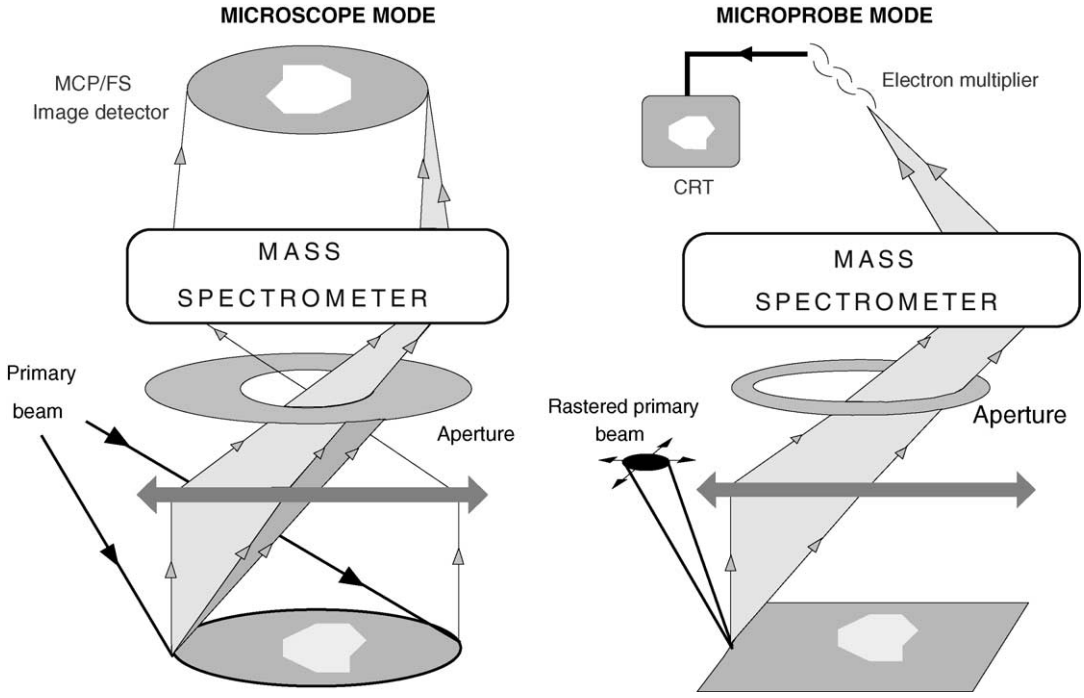

Fig. 2. Operating modes of SIMS [76] (reproduced with permission).

sity, i_p, strikes the sample, collision cascades are initiated, resulting in, among other things, the emission of secondary ions. Not all the ions formed in the source are detected with an instrument transmission, η, as a mass spectrum of ions from an analysed area, A. The detected positive or negative current of an ionic species M at the mass number M will be:

$$I_M = I_p S P_M \eta_M \gamma_M b_M c_e \quad (1)$$

where I_p is equal to $i_p A$ and P is the probability that the particle (atomic or molecular) will emerge as the last step of the sputtering and recombination cascade. S is the sputtering yield (secondary particles per primary ions), γ_M is the positive or negative ionisability of M (ions per atom or molecule), and b_M is the isotopic abundance of M in the element.

2.2.1. Absolute sensitivity

In a situation where the prime goal is to detect trace elements of as low a concentration as possible, without consideration of sample consumption and analytical volume (e.g., in bulk analysis), the suitable figure of merit is the detected secondary ion current of an element A per unit of atomic concentration c(A), that is the absolute sensitivity S_a(A):

$$S_a(A) = \frac{N^q(A)}{c(A)} \quad (2)$$

where N^q is the detected current (in counts per second) of element A in charge state q.

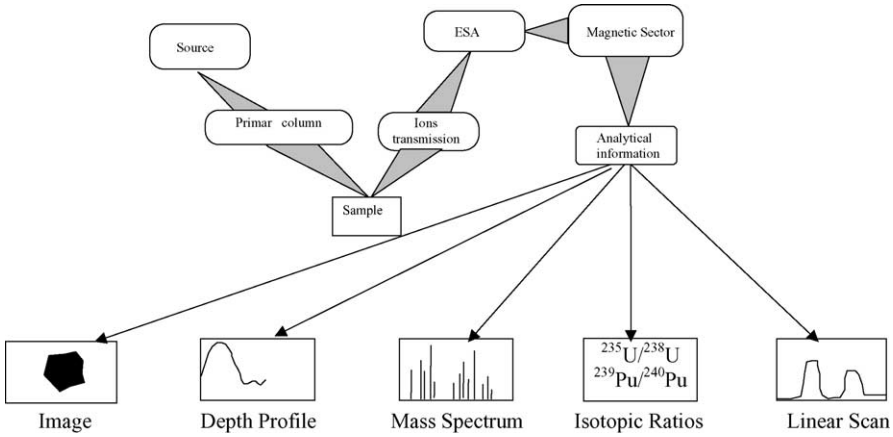

Fig. 3. Analytical information obtainable from SIMS analysis [76] (reproduced with permission).

2.2.2. Practical sensitivity

The practical sensitivity, $S_p(A)$, takes into account the fact that in different analytical situations different primary beam currents may be appropriate:

$$S_p(A) = \frac{N^q(A)}{I_p c(A)} \quad (3)$$

This definition of practical sensitivity does not provide a figure of merit independent of material consumption. The same value would be obtained on different samples for the element A if, at the same primary beam current, the secondary ion currents of element A are identical, even if X sputters much faster than Y.

2.2.3. Useful yield

If the amount of sample is limited or the sampling volume has to be small, the appropriate figure of merit is the *useful yield*, τ_a. It is defined as the number of detected secondary ions/s, $N^q(A)$, of element A per number, $N(A)$, of sputtered A (atoms/s) from the same sampling volume:

$$\tau_a(A) = \frac{N^q(A)}{N(A)} = \frac{S_p(A)}{Y_{tot}} \quad (4)$$

Using the previously introduced figures of merit, the fundamental SIMS formula can be alternatively written as:

$$N^q(A)\,(cps) = S_a(A)c(A) = S_p(A)N_p c(A) = \tau_a(A)N_p Y_{tot} c(A) \quad (5)$$

where S_a is measured in counts per second (cps) and dimensionless units have to be chosen for S_p and τ_a. When S_a, S_p or τ_a are known, Eq. (5) provides a simple means for calculation of elemental concentration, $c(A)$, from the measured secondary particle current, N^q.

Recently the results of an inter-laboratory round robin exercise on the sensitivity of SIMS instruments have been published [11]. The exercise has been performed using metallic uranium and uranium oxide particles as test samples. The practical sensitivity and useful ion yield were measured as comparison parameters. The inter-laboratory standard deviation in the determination of the practical sensitivity was 37% and that of useful ion yield 28%. A good method for optimizing the measurement system and establishing quality control of the SIMS measurements consisted in the determination of practical sensitivity and useful ion yield using standard samples on a daily or weekly basis.

2.2.4. Sensitivity factors

Quantitative results in SIMS can be achieved by external standards or by utilising the concept of sensitivity factors. Under scrupulously reproducible conditions of analysis, and using external standards with composition and microstructures not too different from the analysed samples, useful calibration factors may be obtained. However, long-term instabilities in analysis (instrumental drift, changes in primary beam conditions, vacuum effects, crystalline effects) make the use of absolute sensitivity factors hazardous. It is generally found to be both very feasible and more reliable to utilise the simultaneously measured ion current, I_R, of a matrix reference element, R. The relative sensitivity factor (RSF) of an element A with respect to the element R of the matrix is defined by the following equation:

$$RSF_{A/R} = \frac{N^q(A)/c(A)}{N^q(R)/c(R)} = \frac{S_p(A)}{S_p(R)} \quad (6)$$

This is a very convenient concept since the concentration $c(A)$ of the element A can be calculated from the ratio of the detected ion currents and the known concentration of the reference element in the sample:

$$c(A) = \frac{1}{RSF_{A/R}} \frac{N^q(A)}{N^q(R)} c(R) \quad (7)$$

$RSF_{A/R}$ can be obtained by the measurement (under standard operating conditions) of a single sample with known concentration of elements A and R. The quantitative analysis of a sample containing several elements, using the concept of relative sensitivity factors, can be basically performed without any standard element (reference element with known concentration) if a complete set of relative sensitivity factors for the particular matrix type is available and the total element ion currents of all elements contained in the sample have been measured. In this case the sum concentration can be normalised to 100%, then Eq. (7) can be written:

$$c(X) = \frac{N^q(X)/RSF(X)}{\sum_{i=1}^{N} N^q(X_i)/RSF(X_i)} \quad \text{for all } X \quad (8)$$

It has been found that relative sensitivity factors (RSFs) remain practically constant within quite wide ranges of concentrations, that is, that the differences are only weakly dependent on concentration. Excellent results obtained using RSFs has been reported, for example, for steels, binary alloys, glasses and semiconductors. The dominant sources of variation and irreproducibility in absolute and relative sensitivity factors are connected with the ionisability of the elements.

2.3. Isotope ratio measurements by SIMS

2.3.1. Instrumental parameters and matrix effects

SIMS provides the capability of resolving fine-scale (some μm) isotopic variations within single mineral grains and analysing fine-grained minerals without the need for physical separation. Instrumentation and technical advances have led to improvements in precision to the point where reproducibility is often better than 1‰ and within one to five times that of conventional analysis for H, C, S, B, and O isotopes. These precision levels allow the ion microprobe to be usefully applied to the study of a variety of geological processes, as well as opening new areas of research in cosmochemistry. In fact, during the last 15 years SIMS has been increasingly used for the analysis of light stable isotope ratios in geological and cosmochemical studies [12–17].

However, limitations still restrict the use of the ion microprobe in geological studies. Isotopic fractionation occurs at a variety of stages during SIMS analysis, including sputtering, ionisation, extraction, transmission of the secondary ions through the mass spectrometer, and secondary ion detection. More problematic is the "matrix effect", wherein the chemical composition of the analyte affects measured isotope ratios. The combination of these effects, which almost always favour the light isotope and can result in fractionations of a few to hundreds of per mil from the "true" value, is termed the instrumental mass bias. To obtain accurate isotope ratio measurements the mass bias needs to be adequately quantified and controlled. The correction of mass bias is straightforward when matrix-matched standards are available. However, most matrices are complex, requiring either an extensive suite of standards (that can be time consuming, expensive, and difficult to develop) or predictive models that relate mass bias to sample composition.

Riciputi et al. [18] reviewed the factors that influence instrumental mass bias during SIMS analysis of light stable isotope ratios in minerals focusing primarily on compositional matrix effects. Moreover, they have reviewed empirical models that relate mass bias to matrix composition.

Fitzsimons et al. [19] have reviewed the analytical precision in stable isotope measurements. Assuming that isotope ratios were taken in such a way as to avoid time-fluctuations, the precision was determined by the Poisson counting statistics and SIMS could compete with conventional bulk analysis if counting times of several hours were used. The gradual shift in mass fractionation with time could be corrected for by the analysis of reference materials. The final precision of a corrected isotope ratio largely depended on the scatter in the sample and the reference material.

The introduction of a multicollection system for the Cameca IMS 1270 has been a significant breakthrough towards better measurement reproducibility [20]. However, there are still some limiting instrumental factors preventing one from reaching the desired precision of a few tenths per mil (‰). These instrumental issues are the instrumental mass fractionation variability and the electron multiplier (EM) gain drift (as far as EM detectors are involved) [21]. Schumacher et al. [22] have reported the results of experimental procedure improvements in order to control these two instrumental effects for different types of isotope ratios. They demonstrated that multicollection systems allow improvement of measurement reproducibility for isotope ratios on SIMS instruments provided that the other sources of measurement variability are well controlled. Results for both silicon and oxygen isotopes demonstrate that an experimental error as low 0.2 per mil is achievable whenever both were measured either with Faraday cup detectors or combining one Faraday cup and one electron multiplier (EM).

The introduction of an automatic control of the beam centering for controlling the mass fractionation has significantly improved the measurement reproducibility. For oxygen $^{16}O/^{18}O$ ratio, with a total integration time of 2 min per spot, a STDE (%) of 0.2 per mil has been demonstrated in zircon. A model has been developed to monitor and to apply a post-correction for the EM drift. The pertinence of model has been presented. However, it was found that the EM yield stability is good enough for reaching an experimental precision in the range of 0.2 per mil without need for drift correction.

2.3.2. Applications

2.3.2.1. Geological and cosmogenic applications. Silicon isotopic ratios in a very small area of silicon crystals using a reference silicon crystal are suitable to survey the homogeneity in silicon isotopic compositions of silicon samples. Experiments on crystal growth and silicon isotopic ratio of the silicon crystal have been precisely determined using a SIMS with multicollectors IMS-1270 SIMS [23,24]. The $^{30}Si/^{28}Si$ ratios have been determined and isotopic variations in the range of 1‰ were observed along the growth direction of the crystal. A defocused Cs^+ primary beam was restricted to 40 μm in diameter by a circular aperture to obtain a homogeneous primary beam of about 3 nA. Negative secondary ions of silicon were detected after being uniformly sputtered by a primary beam with a total impact energy of 20 kV. The secondary ^{28}Si, ^{29}Si and ^{30}Si ions were simultaneously detected without energy filtering and using three Faraday cups (FC) of the multicollection system. The internal precision and accuracy in the $^{30}Si/^{28}Si$ ratios (2σ) were better than 0.1 and 0.2‰, respectively.

Oxygen isotopic ratios has been measured by SIMS in several matrices and for different scopes, such as for studying corrosion in power plant boiler tubes [25] or surface oxidation of electrochemically polarised FeCr alloys [26]. Microanalysis of oxygen isotopes has been performed in insulator materials [27] as well as in microparticles [28, see later section dedicated to microparticles] and the matrix effects on oxygen isotope measurements have been systematically investigated in complex minerals and glasses [29]. Oxygen isotope compositions have been reported also for glass inclusions, their host olivines and tholeiitic pillow rim glasses from the neovolcanic rift zone of Iceland. The isotopic heterogeneity of individual olivine crystals allows one to estimate their residence times in the magma reservoir using the rate of ^{18}O diffusion in olivine. Therefore, accurate and precise detection of oxygen isotopic composition is mandatory The inclusion compositions ranged from enriched ($[La/Sm]_n = 1.4–4.8$) to very depleted ($[La/Sm]_n = 0.08–0.35$). The whole rocks and matrix glasses display little variation ($[La/Sm]_n = 0.41–0.51$). Glass inclusions vary somewhat stronger in $^{18}O/^{16}O$ ratios ($\delta^{18}O = 4.0–6.2 \pm 0.6$‰) than the matrix glasses ($\delta^{18}O = 4.6–5.6 \pm 0.6$‰) [30].

Another very important application described in literature [15,16] is the determination of oxygen isotopic composition in meteorites. Chondritic meteorites provide us with direct information about the early history of the solar system. To understand the processes that took place at this time, it is necessary to understand the combined chemical, petrologic, and isotopic information carried by primitive components of

chondrites such as chondrules and calcium-, aluminum-rich inclusions (CAIs). The role of oxygen isotope studies is important to this overall picture because chondritic components record considerable oxygen isotopic complexity that must be unravelled to place chondrule and CAI formation in their appropriate contexts.

In situ oxygen isotope analyses were made for five of the chondrules using the SIMS Cameca IMS 6f ion microprobe, on polished mounts comprising a single chondrule and a San Carlos olivine standard. A 0.2–0.34 nA beam of Cs^+ was focused into a spot ~20 μm in diameter in aperture illumination mode. Secondary ions were collected by peak-jumping into either a Faraday cup ($^{16}O^-$) or electron multiplier ($^{17}O^-$ and $^{18}O^-$) at a mass resolving power of ~6500, easily resolving the $^{16}OH^-$ interference on $^{17}O^-$. Uncertainties on individual analyses, including analytical errors and statistical variation on repeated analyses of the standard, are ~1.5–5‰ (2σ). The magnitudes of matrix effects are small (less than a few ‰) under these analysis conditions therefore no corrections for such effects needed to be performed. [15].

Guan et al. [31] have analysed by SIMS Mg, Cr, and Ni isotopes in primitive meteorites and short-lived radionuclides in the early solar system. By these measurements they have provided evidence for the former existence of ^{26}Al, ^{60}Fe and ^{53}Mn in meteorites (enstatite chondrites) suggesting the abundance of these short-lived radionuclides in the early solar system.

Methods for high-precision measurements of $\delta^{13}C$, $\delta^{15}N$, and N abundance in diamond using a SIMS Cameca 6F ion microprobe have been reported [32,33]. The authors have demonstrated the ability of the technique to provide spatially resolved isotopic data on the scale of the observed growth zoning in diamonds. They paid particular attention to experimental factors which improve the reproducibility and accuracy of the in situ $\delta^{13}C$ and $\delta^{15}N$ measurements.

Belshaw et al. developed a SIMS based techniques for the $^{10}Be/^{9}Be$ ratio measurements in environmental materials [34–36]. The authors described new techniques for Be ionisation, suppression of $^{10}B^+$ and $^{9}BeH^+$ interferences as well as the measurement of $^{10}B/^{9}Be$ by the SIMS VG ISOLAB-120 instrument. The mass resolving power at 5% peak height applied to resolve $^{10}B^+$ from the hydride $^{9}BeH^+$ was about 1400.

$^{207}Pb/^{206}Pb$ SIMS measurements have been performed for dating [37,38]. Ion microprobe measurements of Pb isotope ratios were in situ performed in monazites. Using a resolving power of 6500 molecular interferences were resolved. $^{207}Pb/^{206}Pb$ dating of monazite was obtained with a precision as low as 4–5 Ma (2σ).

Optimized determinations of the isotopic composition of B, C and O with a lateral resolution of 30–50 μm in coral skeletons allowed the pH variations during growth to be assessed with a time resolution as good as 12 h [39]. The isotopes of C and O were measured with a mass resolution of 2000, multicollection detection and Cs^+ primary ions. A mass resolution of 5000, electron multiplier detection and O^- projectiles were used for B isotopes. The internal 1σ error on $^{12}C^-$ and $^{16}O^-$ was ±0.1–0.2‰ and about three times higher for $^{11}B^+$. The average external reproducibility estimated from replicate measurements on carbonate standards over 4 years was ±0.4, 0.65 and 0.9‰ for O, C and B isotopes, respectively. The external reproducibility for O during 1 day was ±0.17‰. The instrumental mass fractionation (IMF), determined by analysis of various carbonate standards, showed a systematic difference between calcite and aragonite of 4.5 and 2.7‰ for C and O, respectively. Duplicate ^{18}O measurements of the same spot in different sessions agreed within 0.5‰. The ion microprobe data showed for B and O much larger isotopic variations at the micrometre scale than those measured at millimetre scale by classical gas source mass spectrometry after phosphoric acid digestion.

2.3.2.2. Imaging measurements of isotope ratios and analysis of biological tissues. Imaging provides an ideal way to study sample heterogeneity because observers intuitively comprehend the variability shown in an image. Secondary ion mass spectrometry can be applied as a powerful tool for imaging measurements of isotope ratios. The spatial resolution can be improved from 0.5 down to about 50–100 nm. The precision can be bettered from 30 to 50‰ down to some tenths.

Fleming and Bekken [40] have used this methodology for $^{34}S/^{32}S$ isotope ratio measurements in pyrite grains in gold ores. The main difficulty in this type of measurements for the ratio $^{34}S/^{32}S$ stems from spreading the already low ^{34}S signal intensity among many pixel. The authors used a CAMECA IMS-4f SIMS. These instruments have a long been noted for their microscopes images in which the position information is stigmatically transferred through the mass spectrometer where it impinges on an image detector. However, they exploited the ion microprobe mode of imaging in their experiments. The ion microprobe electron multiplier accommodates higher secondary ion counts rates than the ion microscope image detectors. Moreover, the ion microprobe mode allows for higher mass resolution and uses lower primary ion beam current, reducing sample charging problems.

Yurimoto et al. [41] have performed high precision $^{18}O/^{16}O$ and $^{17}O/^{16}O$ isotope ratios micro-imaging analysis in minerals using a CAMECA IMS 1270 SIMS. This instrument is a high mass-resolution stigmatic SIMS that provides a mass-filtered stigmatic secondary ion image of the sample surface with a high spatial resolution. Moreover, the authors employed a high-efficiency stacked CMOS-type active pixel sensor (SCAPS) in their experiments. This system has several advantages over conventional detection systems including two-dimensional detection, wide dynamic range, no insensitive period, direct detection of charged particles, and constant ion-detection sensitivities among nuclides. Hence, it can measure high ion flux with an accuracy of within twice the statistical error and with a detection limit corresponding to 10 incident ions.

The identification of the location of individual components at the sub-cellular level is one of the major challenges in medicine and biology. Proteins can often be located in fixed (i.e., dead) material using specific antibodies for microscopy or in living tissues using laser confocal microscopy using specific fluorescence labels.

Chandra and Morrison [42] have exploited the imaging technique to study molecular transport mechanisms at sub-cellular resolution. For example, $^{44}Ca/^{40}Ca$ isotope ratios have been measured to study the transport of ^{44}Ca into the interior of the cells under physiological and pathological conditions. This capability of SIMS provides a unique and powerful approach for understanding the role of calcium in cell physiology. Similarly, ion transport studies of other elements can be performed with stable isotopes.

Recently, Chandra et al. [43] reviewed the sub-cellular imaging of biological samples, for which application SIMS evolved as a viable alternative to the commonly used electron microprobe. The feasibility of pixel-by-pixel quantification by means of RSF referenced for example, to the cell matrix carbon was demonstrated. Isotopic detection was considered a major asset, which allowed stable, non-radioactive tracers to be used to study transport phenomena or to localise drugs and metabolites. The most critical step in sub-cellular ion and molecular localisation studies with SIMS is the sample preparation. Due to the high vacuum requirements of SIMS, live cells cannot be analysed. Therefore, cells must be preserved in their native state so that the analysis reveals the chemical makeup of the living cells. This poses a classical problem for SIMS analysis as well as in all surface techniques.

The distribution of sulphur has been studied in wheat starchy endosperm cells [44]. Analysis of the distributions of ^{32}S and ^{34}S from their images revealed that both isotopes were clearly concentrated at the starch granule surface and the interface between the granules and the matrix proteins. Analysis of the signal strengths of isotopes ^{32}S, ^{34}S and ^{16}O in different parts of the endosperm cells showed a higher concentration of ^{34}S at the outer surfaces of the starch granules compared to the cut interior faces of the structures. The protein matrix also had a lower concentration in ^{34}S isotope than the starch granules.

Cliff et al. [45,46] focused their research on developing TOF-SIMS to measure organic ^{15}N in biological and environmental samples. They developed a peak-fitting algorithm that removes the isobaric interferences of Al^- and $^{13}C^{14}N^-$ from $^{12}C^{15}N^-$ ions under conditions of low mass resolution.

Grignon et al. [47] determined the local concentrations of a ^{15}N tracer in soybean leaf samples, using carbon and the natural isotope ratio of N in the embedding medium to standardise the instrumental conditions. Detection of CN^- allowed R.S.D. within 10% to be obtained and the measured concentrations agreed within 20% with bulk mass spectrometry analysis.

2.3.2.3. Single micro-particles. Single particles in the 1–10 μm range remains a challenging application of SIMS.

Nittler and Alexander [48] developed an analytical system for the fully automated determination of isotopic ratios in μm-sized particles on the basis of ion imaging and new algorithms to localise the particles. A 75 μm × 75 μm or 150 μm × 150 μm sample area were scanned with a Cs^+ or O^- primary ion beam, focused to a spot with diameter of 1 or 0.5 μm, respectively. Once localised, the particles of interest were then individually analysed with a focused ion beam scanned over an area of 3 μm × 3 μm. Use of optical encoders circumvented the poor reproducibility of the commercial sample stage and positioned the beam within 1 μm of a predefined point. The statistical error on ^{28}Si and ^{29}Si using the peak-jumping mode was 2.6 and 2.7‰, respectively, while the intrinsic uncertainty remained within 3‰/amu for Si isotopic ratios. The automated analysis typically processed 300 particles per day, depending on the number of grains per area and their size.

Betti et al. [49,50] used SIMS for the characterisation of plutonium and highly enriched uranium in nuclear forensic analysis. They measured the uranium isotopic composition with a typical accuracy and precision of 0.5%. As for Pu, the isotopic ratio 239/240 was determined and resulted in agreement with the results from thermal ionisation mass spectrometry. The same authors have measured $^{18}O/^{16}O$ isotope ratio by SIMS in uranium oxide microparticles [28] for nuclear forensic diagnostic. The same group [51] has exploited SIMS, in combination with other instrumental analytical techniques, for the characterisation of soil particles bearing depleted uranium (DU). The particles localised by the automated SEM with gun shot residue program were then analysed by SIMS for uranium isotopic ratios. They clearly contain DU, and traces of ^{236}U were also detected. As for ^{234}U and ^{236}U, due to the low signal intensity the error is often larger. In general, the total uncertainty on the minor isotopes is decreasing (better counting statistics) when the enrichment increases. The uncertainty on the ^{236}U is significantly higher than that on the ^{234}U, because the 236 intensity is obtained after correction for hydride contribution and the respective errors are propagated into the 236 uncertainty. With such a particle diameter (≈1 μm), the precision that can be achieved is considered the detection limit of the method in these conditions. The signal on mass 239 (due only to the formation of $^{238}UH^+$ molecules) is used to correct the signal on mass 236 for the contribution of $^{235}UH^+$. As for ^{235}U in this case the uncertainty is not strongly depending on the intensity of the signal but from other parameters, e.g., the analysis time.

3. Glow discharge mass spectrometry

Glow discharge mass spectrometry (GDMS) consists of the coupling of a glow discharge atomisation/ionisation source with a mass spectrometer. As noted earlier, the relative simplicity of mass spectra compared with optical spectra makes mass spectrometry an attractive alternative to opti-

cal spectrometry for trace element analysis. Moreover, mass spectrometry permits the coverage of essentially the entire periodic table and, since the spectral background can be very low, detection limits are usually two to three orders of magnitude better by mass spectrometry than for optical atomic emission using a glow discharge.

For over 50 years glow discharges have been known as ion sources for mass spectrometry. The capability of generating a stable analyte ion population directly from a solid sample, thereby precluding the problems of dissolution, dilution and contamination that may arise for techniques requiring solution samples, makes the glow discharge an attractive ion source for elemental mass spectrometry of solids. The ability to obtain isotopic information across the periodic table down to ng g^{-1} detection limits, along with the developments of improved mass spectrometers with more reliable data acquisition and control systems, has made GDMS a powerful tool, not only for research laboratories but also for routine applications.

A wide variety of analytical glow discharge geometries have been investigated as ion sources. Most GD sources, particularly the commercial versions, have used a direct insertion probe that permits certain flexibility in sample shape, although pins or discs are normally used. In this configuration, the sample serves as the cathode of the glow discharge system and the cell housing as the anode. Ions are sampled from the negative glow region through an exit orifice. In Table 1, a comparison of the different sources is given. Hollow cathode glow discharges were coupled with a magnetic sector analyser in preliminary investigations of analytical GDMS [52]. Commercial instruments employ a modified coaxial cathode geometry [53] the so-called "pin-type" glow discharge source. This is also the most widely characterised glow discharge ion source.

Whereas different glow discharge ion sources have not exhibited any significant performance differences, different methods of powering the sources show specific performance differences. The dc-powered sources are the most common, even though RF-powered sources have been studied [54] and applied as well as the pulsed sources [55]. Recently, Winchester and Payling [56] have critically reviewed radio-frequency glow discharge spectrometry.

The most widely used commercial GDMS instrument is the VG9000 that consists of a dc-powered source, a double-focusing mass analyser of the reverse Nier–Johnson geometry and Daly and Faraday cup detectors.

3.1. Glow discharge processes

A glow discharge is a partially ionised gas consisting of approximately equal concentrations of positive and negative charges plus a large number of neutral species. It consists of a cathode and anode immersed in a low-pressure (≈0.1–10 Torr) gas medium. Application of an electric field across the electrodes causes breakdown of the gas (normally one of the rare gases is used, typically argon) and the acceleration of electrons and positive ions towards the oppositely charged electrodes. Detailed description of the phenomena can be found in [57–59]. As an ion source for elemental mass spectrometry, the glow discharge is characterised by two attractive attributes, cathodic sputtering and Penning ionisation, that are inherent to its operation. Cathodic sputtering generates a representative atomic population directly from the solid sample. Penning ionisation selectively ionises these sputtered atoms, permitting detection on the basis of their characteristic mass-to charge ratios by mass spectrometry.

3.1.1. Atomisation

Cathodic sputtering is the phenomenon that makes a glow discharge useful in analytical spectrometry, providing the means of obtaining directly from a solid sample an atomic population for subsequent excitation and ionisation. The sputtering involves collisions of energetic particles onto a surface where, after collision, it transfers its kinetic energy in a series of lattice collisions. Atoms near the surface can receive sufficient energy to overcome the lattice binding and be ejected, generally as neutral atoms with energies in the range of 5–15 eV. The bombarding particles are normally ions, easily accelerated by electrical fields that are inherent to the GD plasma. The sputter yield, defined as the number of ejected atoms per bombarding ion, depends critically on the mass and energy of the incoming ions. Under the operating conditions of most analytical glow discharges, the sputter yield can be described as a function of kinetic energy and mass of

Table 1
Comparison of glow discharge sources

Source	Voltage (V)	Current (mA)	Pressure (Torr)	Cathode	Advantages	Disadvantages
Hollow cathode	200–500	10–100	0.1–1.0	23 mm deep cylinder with 5 mm diameter base	High sputter; intense ion beams; useable for powders	Charge exchange mechanisms are important; complicated sample geometry
Grimm	500–1000	25–100	1–5	6.5 mm diameter circle	Depth profiling; easy for compacted powders	Only flat samples; higher discharge gas flow rates
Jet-enhanced	900	28	2.5	12 mm diameter circle	High sputter rate; easy for compacted powders	Only flat samples; higher discharge gas flow rate
Coaxial cathode	800–1500	1–5	0.2–2.0	1.5–2.0 mm diameter × 4–8 mm long rod	Useable for various sample shapes; ionisation dominated by Penning process	Powders need to be converted into solid samples

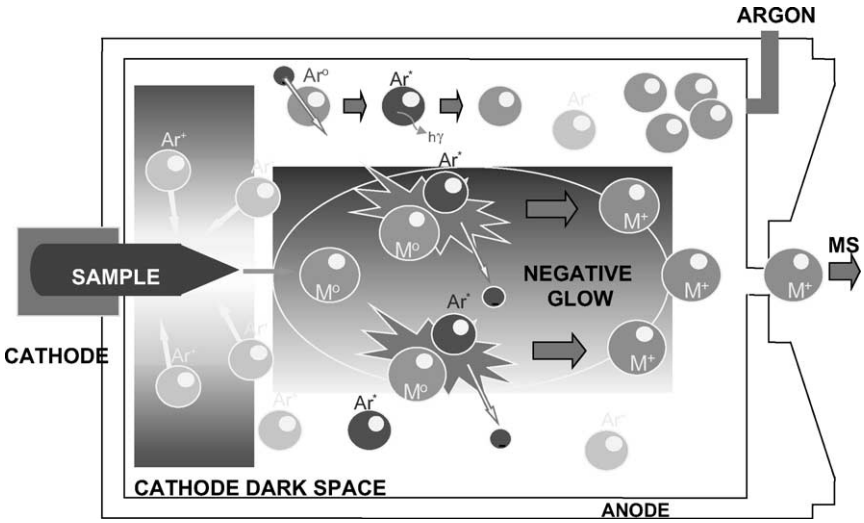

Fig. 4. Processes in a glow discharge source.

the bombarding atom as well as of the lattice binding energy and mass of the target atoms. A related value is the sputtering rate, namely the amount of material sputtered per unit time. This value is determined by the discharge operating current as well as the factors affecting the sputter yield.

3.1.2. Ionisation

The glow discharge sputtering can introduce into the plasma a representative population of the sample (cathode) atoms. A fraction of them needs to be ionised for further elemental analysis by mass spectrometry. The discharge must then act as ionising medium and must, of course, sustain itself. The fact that GDMS does not utilise optical transitions of the analyte atoms, rather the mass-to-charge ratio of the atoms that have been ionised, shifts the emphasis from excitation mechanisms to ionisation mechanisms, simplifying, to some extent, the relationship between analyte signal and analyte concentration in the sample. Fig. 4 shows schematically the processes in a GD and in Table 2 ionisation processes in glow discharges are summarised.

Whereas we can assume that atomisation does not differ significantly between elements in a given matrix, we cannot assume the same to be true for ionisation. Therefore, relative sensitivity factors (RSFs) used for quantitative analysis are most likely controlled by differences in the probability of ionisation among the elements. The RSF of an analyte element, A, is the ratio of its sensitivity to the sensitivity of some reference element. Sensitivity is defined as the intensity (I) of the signal per unit of concentration (C):

$$\mathrm{RSF}_{\mathrm{A/R}} = \frac{I_{\mathrm{A}}/C_{\mathrm{A}}}{I_{\mathrm{R}}/C_{\mathrm{R}}} \tag{9}$$

The RSFs consider the contributions arising from instrumental factors, such as ion transmission and sensitivity, and glow discharge processes, such as differential atomisation and differential ionisation. The dominant contribution is related to the glow discharge processes and varies from sample to sample.

Table 2
Ionisation process in the glow discharge

Electron impact ionisation[a]	$A + e^- \rightarrow A^+ + 2e^-$
Penning ionisation[b]	$Ar^m + X \rightarrow Ar + X^+ + e^-$
Associative ionisation[b]	$Ar^m + X \rightarrow ArX^+ + e^-$
Symmetric charge exchange[b]	$A^+ + A \rightarrow A + A^+$
Asymmetric charge exchange[b]	$A^+ + B \rightarrow A + B^+$

[a] Collisions of the first kind.
[b] Collisions of the second kind.

3.2. Quantification

The mass spectrum obtained by GDMS can be used directly for a semiquantitative measurement of the sample composition. One method is based on the ion-beam ratio (IBR) [60]. In this procedure, the ion signals for all ionised sputtered species are summed and then the ratio of the ion signal for individual species is calculated, which corresponds to the concentration of the species in the bulk. Since the ion beam ratio depends on the sensitivity of the different elements, which varies by less than a factor of ten, this method can only provide reliable means for semiquantitative analysis.

The signal intensity of the plasma species is influenced by several factors. Among these are: sample composition, matrix type, discharge power, cathode geometry, cooling effects, discharge gas, source pressure, ion transmission, the type of mass spectrometer and the detection system. Because of all this, for quantitative analysis, the use of standards is required for calibration. This can be performed in two ways. The first consists of the construction of a calibration curve, based on a set of similar standards [61,62]. The second possibility is based on the analysis of a reference material as similar as possible in composition and behaviour to the unknown sample, which allows the calculation of the relative sensitivity factors (RSFs) [63]. Since suitable certified standards are not always

available, powdered samples may be doped with an element of known concentration to be used as an internal standard. In order to yield the ion beam ratios are corrected by the RSFs values. Namely, the use of a good standard, the measurements of the IBRs, and correcting them for RSFs, provides the best quantification procedure.

3.3. Applications to trace element analysis

GDMS has taken the place of spark source mass spectrometry (SSMS) for the analysis of trace elements in solid samples. In comparison to SSMS, GDMS presents many advantages, for instance, a simple source producing a stable supply of low energy ions characteristic of the sample and minimal matrix effects.

In a dc-powered GDMS instrument, the samples must be conductive; therefore, bulk metals are the most ideal samples even though non-conductive samples can also be analysed. In this case, the samples need to be mixed with a binder material [63] (Ag, Ti or Ta) or the technique of the secondary cathode can be applied [64]. Sample spectra may be obtained in a short time (min) and rapid qualitative analysis can be performed by the examination of the isotopic lines. Quantitative analysis can also be achieved, as previously explained.

Semiconductors are another important category of bulk samples that can be analysed by GDMS. The electrical properties of these materials are critically dependent on the intrinsic and doped levels of impurities, making it essential to know, not only qualitatively their chemical composition, but also the concentration level of each element. Even extremely low concentrations of a specific element can alter semiconductor properties.

GDMS is always a surface analysis technique, even though it permits measurement of bulk concentrations. That is, the sputtering process central to the glow discharge acts as an atomic mill that regularly erodes away the surface of the bombarded sample. Whatever atoms are sputtered away from the surface are measured and, because GDMS consumes significant quantities of material (up to milligrams per minute), these sequential layer analyses combine to yield an averaged composition that is typical of the bulk concentration. By slowing down the ablation process limiting measurement to a shorter duration, data indicative of the surface concentrations can be obtained. GDMS and its optical analogue have found considerable application for the analysis of layered samples.

Environmental samples can be also analysed by GDMS. In these cases the samples need to be compacted with or without conducting material [65]. Where a binder of conducting material is not added during the compaction of the samples, a secondary cathode can be employed.

3.4. Isotope ratio measurements by GDMS

GDMS has also been exploited for the determination of the isotopic composition in samples of nuclear concern [66].

Lithium and boron are light elements having two natural isotopes whose abundances are widely different: ^{6}Li (7.5%), ^{7}Li (92.5%), ^{10}B (19.9%) and ^{11}B (80.1%). Their detection in nuclear material is important for the determination of its purity. Boron is a neutron capture element and lithium is used as a doping additive. The most widely used method for their isotopic abundance determination is TIMS, after sample dissolution. The use of ICP-MS is hindered by its low detection power for light elements. By GDMS, detection at the ng g^{-1} levels is easily achievable.

As to boron, at mass 10 the interference caused by the formation of $^{40}Ar^{4+}$ occurs. According to the sample matrix, $^{40}Ca^{4+}$ and $^{30}Si^{3+}$ are also formed. The necessary mass resolution to separate ^{10}B from all these interferences is equal to 500. As for lithium interferences on $^{6}Li^{+}$ and $^{7}Li^{+}$ can arise from $^{12}C^{2+}$ and $^{14}N^{2+}$, respectively. Also in these cases the minimum resolution necessary for separation is 500.

Chartier and Tabarant [67] have also performed isotopic measurements directly on solid samples of ZrB by HR-GDMS. By this way they could resolve the interference $^{40}Ar^{4+}$ from $^{10}B^{+}$, that was not possible by a quadrupole GDMS. The authors compared the accuracy and the precision of the HR-GDMS based method with those figures obtained by TIMS. The instrumental mass discrimination determined for HR-GDMS was 1.4%; the internal precision obtained varied from 0.2 to 0.5%. The external precision was of 0.3%.

Silicon isotopic composition in aluminium matrices has been also determined by GDMS [68]. The determination of silicon concentration cannot be accomplished by the worldwide employed quadrupole based inductively coupled plasma mass spectrometers (ICP-MS). The resolution required for the separation of $^{28}Si^{+}$ from $^{12}C^{16}O^{+}$ and $^{14}N_2{}^{+}$ is 1625 and 957, respectively. Moreover, in an aluminium matrix the tail of Al and the formation of $^{27}AlH^{+}$ produce also interferences on $^{28}Si^{+}$ that cannot easily be resolved. The other two isotopes of silicon have a low abundance: 4.67% for ^{29}Si and 3.10% for ^{30}Si, and a high detection power must be reached to obtain accurate isotopic compositions. The dissolution of those type of sample is tedious and sometimes, due to presence of other metals, incomplete. Double-focusing GDMS can be used successfully for the measurement of silicon isotopic abundance. On $^{28}Si^{+}$ the interferences due to formation of $^{27}AlH^{+}$, $^{12}C^{16}O^{+}$ and $^{14}N_2{}^{+}$ can be easily resolved as well as those interferences due to $^{28}SiH^{+}$, $^{27}AlH_2{}^{+}$ and $^{12}C^{16}OH^{+}$ on $^{29}Si^{+}$ and that due to $^{14}N^{16}O^{+}$ on $^{30}Si^{+}$. $^{27}AlH^{+}$ comes together with $^{12}C^{16}O^{+}$ as well as the $^{27}AlH_2{}^{+}$ with $^{12}C^{16}OH^{+}$. $^{27}AlH_3{}^{+}$ should appear at mass 30.005, but no evidences for its formation appeared. $^{28}SiH^{+}$ and $^{14}N^{16}O^{+}$ resulted to be well separated from $^{29}Si^{+}$ and $^{30}Si^{+}$, respectively. Five aluminium samples containing traces of silicon were measured using a mass resolution of 2000, and for each sample ten separate runs were carried out. The precision (expressed as R.S.D.%) and the accuracy (expressed as bias%) of the mean values obtained for the three isotopes were about 1 and 0.2%, respectively. Many samples containing uranium with different isotopic composition have been measured [66]. When the

results of the isotope ratios obtained by GDMS and TIMS were compared for the four isotopes of uranium, included the non-natural ^{236}U, a good agreement was always found. The advantage of the use of GDMS is omission of the time-consuming dissolution and dilution steps.

Glow discharge optogalvanic spectroscopy has been investigated for the determination of uranium and actinide isotope ratios [68–70]. In these investigations, a hollow cathode glow discharge has been coupled with a tunable laser for isotopically selective excitation of gaseous uranium atoms produced by cathodic sputtering. In a glow discharge, the cathode bombarded by energetic ions produces a population of gaseous ions directly amenable to isotopic analysis by a mass spectrometer. Neutrals are also produced that are amenable for detection in a variety of other techniques, like absorption, emission, and laser-induced fluorescence spectroscopy. In the investigation performed by Young et al. [68], the sputtered atoms are resonantly excited to a higher lying energy level, from which they may be ionised by collision. The change in the discharge voltage brought about by disruption of the ionisation equilibrium serves as an indicator of optical absorption and is the basis of optogalvanic signal collection. The instrumentation developed had as a final goal to be applied in field. For this application accuracy and precision of the same level than a laboratory mass spectrometer are generally not required. However, sensitivity to changes of the isotopic composition, free from interferences, is of high importance. The authors evaluated the measurement precision and accuracy uranium isotopic composition and found that for depleted uranium the precision of the isotope ratios was ±15% and for enriched uranium of ±3%. The method can be used for a rapid and inexpensive screening and has been applied for the determination of uranium isotope ratios in different sample matrices as uranium oxide, fluoride and metal [70].

Barshick et al. [71] has applied flow-discharge Fourier-transform ion cyclotron resonance mass spectrometry to isotope ratio measurements of lead: $^{206}Pb/^{208}Pb$, $^{207}Pb/^{208}Pb$, $^{207}Pb/^{206}Pb$.

The increasing interest in isotopic composition studies and ultra-low level (abundance below 10^{-10}) radionuclide metrology for a variety of applications in environmental and biomedical applications led to the development of a continuous-wave resonance ionisation mass spectrometer (cw-RIMS) system at the National Institute of Standards and Technology [72–74]. Resonance ionisation mass spectrometry (RIMS) can determine ultratrace levels of a single isotope of a particular element in a sample. The laser excitation scheme of RIMS increases the isotopic selectivity obtained by standard mass spectrometry and eliminates isobaric interferences. The NIST cw-RIMS consists of three major parts: a sample loading system (glow discharge or graphite furnace) as the atom source, a continuous wave laser system to ionise the atoms, and a mass spectrometer to analyse and detect the resulting ions. The apparatus can simultaneously produce copious amounts of atoms for analysis while not interfering with the high-vacuum conditions required for accurate mass spectrometric analysis. A glow discharge method to introduce a sample to the cw-RIMS system (GD-RIMS) with a magnetic sector analyser has been successfully tested on caesium by Pibida et al. [72]. This method involved selective laser ionisation, with one-step laser excitation scheme. Careful atomic beam collimator and alignment of the lasers with respect to the atomic beam reduce the Doppler broadening thereby increasing the laser ionisation selectivity and ionisation efficiency. The overall efficiency namely the number of detected ions divided by the total number of atoms emitted, was measured to be 10^{-8} while the selectivity (the detectable ratio between adjacent isotopes based on mass) was estimated to be between 10^9 and 10^{10} from which, a factor of 10^3 was estimated to be the enhanced selectivity due to single-step laser excitation followed by ionisation. With this set-up of the GD-RIMS, the system could be used to determine trace amounts of radionuclides, with half-lives in the 10^5 years range, at normal environmental levels and with a minimum of chemical preparation.

In the last years, Laser ablation ICPMS has been applied for the determination of long-lived radionuclides and their isotopic composition [1,4,75]. The method appears to be very competitive with the GDMS one and it would be worthwhile to analyse the samples with both techniques for validation of results for quality control/quality assurance purposes.

4. Summary

Nowadays both SIMS and GDMS are well-established techniques for the characterisation of solid samples.

GDMS is a powerful tool for bulk measurements of major, minor and trace elements. Moreover, it can be successfully applied for accurate isotope ratio measurements in a large variety of matrices. The combination of GD with RIMS can help to solve isobaric interferences at the solid state.

SIMS can be usefully exploited for investigating micro-inclusions in bulk materials as well as for the characterisation of microparticles. Its emerging and promising applications for isotopic ratio measurements are in the field of cosmochemistry, geochemistry, biology and forensic analysis. One of its major features that merits to be more exploited is the imaging method for isotopic ratio measurements.

Both techniques have the capability of depth profiling, however, GDMS can perform with a deeper penetration of the surface. On the other hand SIMS can carry out surface profile (linear scan) with a micrometer later resolution.

Used in combination, GDMS and SIMS can give a complete characterisation of the sample as for the isotopic ratios as well as quantitative analysis at the solid state.

References

[1] J.S. Becker, J. Anal. Atom. Spectrom. 17 (2002) 1172.

[2] J.R. Bacon, J.S. Crain, L. van Veck, J.G. Williams, J. Anal. Atom. Spectrom. 16 (2001) 879.
[3] J.R. Bacon, J.C. Greenwood, L. Van Vaeck, J.G. Williams, J. Anal. Atom. Spectrom. 19 (8) (2004) 1020.
[4] J.S. Becker, Spectrochim. Acta B 58 (2003) 1757.
[5] M. Betti, L. Aldave de las Heras, Spectrochim. Acta B 59 (2004) 1359.
[6] J.S. Becker, H.-J. Dietze, Int. J. Mass Spectrom. 197 (2000) 1.
[7] G. Huber, G. Passler, K. Wendt, J. Volker, N. Trautmann, in: M.F. L'Annunziata (Ed.), Handbook of Radioactivity Analysis, 2nd ed., Academic Press, New York, 2003, p. 799.
[8] L. Ebdon, A.S. Fisher, M. Betti, M. Leroy, in: Z. Mester, R. Sturgeon (Eds.), Comprehensive Analytical Chemistry, vol. XLI, Wilson & Wilson/Elsevier Science Publisher, 2003, p. 117.
[9] R.K. Marcus, J.A.C. Broekaert, Glow Discharges Plasmas in Analytical Spectroscopy, John Wiley & Sons, Chichester, 2003.
[10] A. Benninghoven, F.G. Rüdenauer, H.W. Werner, Secondary Ion Mass Spectrometry: Basic Concepts, Instrumental Aspects applications and Trends, Wiley, New York, 1987.
[11] G. Tamborini, D.L. Donohue, F.G. Rüdenauer, M. Betti, J. Anal. Atom. Spectrom. 19 (2) (2004) 203.
[12] L.R. Riciputi, D.R. Cole, H.G. Machel, Geochim. Cosmochim. Acta 60 (1996) 325.
[13] I.C. Lyon, J.M. Saxton, P.J. McKeever, E. Chatzitheodoridis, P. Van Lierde, Int. J. Mass Spectrom. Ion Process. 9 (1995) 1.
[14] L.A. Leshin, A.E. Rubin, K.D. McKeegan, Geochim. Cosmochim. Acta 61 (1997) 835.
[15] E. Deloule, F. Allegre, S.M.F. Sheppard, Earth Planet. Sci. Lett. 105 (1991) 543.
[16] R.H. Jones, L.A. Leeshin, Y. Guan, Z.D. Sharp, T. Durakiewicz, A.J. Schilk, Geochim. Cosmochim. Acta 68 (2004) 3423.
[17] M. Ito, H. Nagasawa, H. Yurimoto, Geochim. Cosmochim. Acta 68 (2004) 2905.
[18] L.R. Riciputi, B.A. Paterson, R.L. Ripperdan, Int. J. Mass Spectrom. 178 (1998) 81.
[19] I.C.W. Fitzsimons, B. Harte, R.M. Clark, Miner. Mag. 64 (1) (2000) 59.
[20] E. de Chambost, F. Fercocq, F. Fernandes, E. Deloule, M. Chaussidon, Proceedings of the International Conference on SIMS, vol. XI, Wiley, 1997.
[21] G. Slodzian, et al., EPJ Appl. Phys. 14 (3) (2001) 199.
[22] M. Schumacher, F. Fernandes, E. de Chambost, Appl. Surf. Sci. 231/232 (2004) 878.
[23] Y. Morishita, H. Satoh, Appl. Surf. Sci. 203/204 (2003) 802.
[24] Y. Morishita, H. Satoh, Appl. Surf. Sci. 231/232 (2004) 907.
[25] D.R. Cole, l.R. Riciputi, D.J. Wesolowski, B.A. Paterson, S.M. Fortier, Corros. Sci. 39 (1997) 2215.
[26] C. Courty, H.J. Mathieu, D. Landolt, Electrochim. Acta 36 (1991) 1623.
[27] R.L. Hervig, P. Williams, R.M. Thomas, S.N. Schauer, I.M. Steele, Int. J. Mass Spectrom. Ion Process. 120 (1992) 45.
[28] G. Tamborini, D. Phinney, O. Bildstein, M. Betti, Anal. Chem. 74 (2002) 6098.
[29] J.M. Eiler, C. Graham, J.W. Valley, Chem. Geol. 138 (1997) 221.
[30] A.A. Gurenko, M. Chaussidon, Earth Planet. Sci. Lett. 205 (2002) 63.
[31] Y. Guan, G.R. Huss, L.A. Leshin, Appl. Surf. Sci. 231/232 (2004) 899.
[32] E.H. Hauri, J. Wang, D.G. Pearson, G.P. Bulanova, Chem. Geol. 185 (2002) 149.
[33] G.P. Bulanova, D.G. Pearson, E.H. Hauri, B.J. Griffin, Chem. Geol. 188 (2002) 105.
[34] N.S. Belshaw, R.K. O'Nions, F. von Banckenburg, Int. J. Mass Spectrom. Ion Process. 142 (1995) 55.
[35] F. von Banckenburg, N.S. Belshaw, R.K. O'Nions, Chem. Geol. 129 (1996) 93.
[36] F. von Banckenburg, R.K. O'Nions, N.S. Belshaw, A. Gibb, J.R. Hein, Earth Planet. Sci. Lett. 141 (1996) 213.
[37] C.P. DeWolf, N. Belshaw, R.K. O'Nions, Earth Planet. Sci. Lett. 120 (1993) 207.
[38] C. Pomiès, B. Hamelin, J. Lancelot, R. Blomqvist, Appl. Geochem. 19 (2004) 273.
[39] C. Rollion-Bard, M. Chaussidon, C. France-Lanord, Earth Planet. Sci. Lett. 215 (1/2) (2003) 275.
[40] R.H. Fleming, B.M. Bekken, Int. J. Mass Spectrom. Ion Process. 143 (1995) 213.
[41] H. Yurimoto, K. Nagashima, T. Kunihiro, Appl. Surf. Sci. 203/204 (2003) 793.
[42] S. Chandra, G.H. Morrison, Int. J. Mass Spectrom. Ion Process. 143 (1995) 161.
[43] S. Chandra, D.R. Smith, G.H. Morrison, Anal. Chem. 72 (3) (2000) 104A.
[44] K.A. Feeney, P.J. Heard, F.J. Zhaog, P.R. Shewry, J. Cereal Sci. 37 (2003) 311.
[45] J.B. Cliff, D.J. Gaspar, P.J. Bottomely, D.D. Myrold, Appl. Environ. Microbiol. 68 (2002) 4067.
[46] J.B. Cliff, D.J. Gaspar, P.J. Bottomely, D.D. Myrold, Appl. Surf. Sci. 231/232 (2004) 912.
[47] N. Grignon, J. Jeusset, E. Lebeau, C. Moro, A. Gojon, P. Fragu, J. Trace Microprobe Tech. 132 (1999) 477.
[48] L.R. Nittler, C.M.O. Alexander, Geochim. Cosmochim. Acta 67 (24) (2003) 4961.
[49] G. Tamborini, M. Betti, Mikrochim. Acta 132 (2–4) (2000) 411.
[50] M. Betti, G. Tamborini, L. Koch, Anal. Chem. 71 (1999) 2616.
[51] S. Török, J. Osán, L. Vincze, S. Kurunczi, G. Tamborini, M. Betti, Spectrochim. Acta B 59 (2004) 689.
[52] B.N. Colby, C.A. Evans, Anal. Chem. 46 (1974) 1236.
[53] W.W. Harrison, C.M. Barshisk, J.A. Klingler, P.H. Ratliff, Y. Mei, Anal. Chem. 62 (1990) 943A.
[54] C.R. Schick, P.A. De Palma, R.K. Marcus, Anal. Chem. 68 (1996) 2113.
[55] W.W. Harrison, W. Hang, J. Anal. Atom. Spectrom. 11 (1996) 835.
[56] M.R. Winchester, R. Payling, Spectrochim. Acta B 59 (2004) 607.
[57] W.W. Harrison, in: F. Adams, R. Gijbels, R. van Grieken (Eds.), Inorganic Mass Spectrometry, John Wiley & Sons, 1988.
[58] L. King, W.W. Harrison, in: R.K. Marcus (Ed.), Glow Discharge Spectroscopies, Plenum Press, New York, 1993.
[59] W.W. Harrison, C. Yang, C. Oxley, in: R.K. Marcus, J.A.C. Broekaert (Eds.), Glow Discharge Plasma in Analytical Spectroscopy, John Wiley & Sons, 2003.
[60] R.W. Smithwick, J. Am. Soc. Mass Spectrom. 3 (1992) 79.
[61] C.L. Yang, M. Mohill, W.W. Harrison, J. Anal. Atom. Spectrom. 15 (2000) 1255.
[62] L. Aldave de las Heras, E. Hrnecek, O. Bildstein, M. Betti, J. Anal. Atom. Spectrom. 11 (2002) 1011.
[63] M. Betti, J. Anal. Atom. Spectrom. 11 (1996) 855.
[64] A. Bogaerts, W. Schelles, R. van Grieken, in: R.K. Marcus, J.A.C. Broekaert (Eds.), Glow Discharge Plasma in Analytical Spectroscopy, John Wiley & Sons, 2003.
[65] M. Betti, S. Giannarelli, T. Hiernaut, G. Rasmussen, L. Koch, Fresenius J. Anal. Chem. 355 (1996) 642.
[66] M. Betti, G. Rasmussen, L. Koch, Fresenius J. Anal. Chem. 355 (1996) 808.
[67] F. Chartier, M. Tabarant, J. Anal. Atom. Spectrom. 12 (1997) 1187.
[68] J.P. Young, R.W. Shaw, C.M. Barshick, J.M. Ramsey, J. Alloys Compd. 271–273 (1998) 62.
[69] C.M. Barshick, R.W. Shaw, J.P. Young, J.M. Ramsey, Anal. Chem. 67 (1995) 3814.
[70] C.M. Barshick, R.W. Shaw, J.P. Young, J.M. Ramsey, Anal. Chem. 66 (1994) 4154.

[71] C.M. Barshick, k.L. Goodner, C.H. Watson, J.R. Eyler, Int. J. Mass Spectrom. 178 (1998) 73.
[72] L. Pibida, J.M.R. Hutchinson, J. Wen, L. Karam, Rev. Sci. Instrum. 71 (2) (2000) 509.
[73] L. Pibida, W. Nörtershäuser, J.M.R. Hutchinson, B.A. Bushaw, Radiochim. Acta 88 (2000) 1.
[74] L.R. Karam, L. Pibida, C.A. McMahon, Appl. Radiat. Isotopes 56 (2002) 369.
[75] J.S. Becker, C. Pickardt, H.-J. Dietze, Int. J. Mass Spectrom. 203 (2000) 283L 297.
[76] G.T. Tamborini, PhD Thesis, University of Paris-Sud, Orsay, France, 1998.